Title

Evaluation of bound and pore water in cortical bone using ultrashort-TE MRI

Journal

NMR in Biomedicine, 28(12)

ISSN

0952-3480

Authors

Chen, Jun

Grogan, Shawn P

Shao, Hongda

et al.

Publication Date

2015-12-01

DOI

10.1002/nbm.3436

HHS Public Access

Author manuscript

NMR Biomed. Author manuscript; available in PMC 2016 December 01.

Published in final edited form as:

NMR Biomed. 2015 December ; 28(12): 1754–1762. doi:10.1002/nbm.3436.

Evaluation of Bound and Pore Water in Cortical Bone Using Ultrashort Echo Time (UTE) Magnetic Resonance Imaging

Jun Chen, Ph.D.[#1,2], **Shawn P Grogan, Ph.D.**[#3], **Hongda Shao, M.S.**[2], **Darryl D'Lima, M.D., Ph.D.**[3], **Graeme M Bydder, M.B.Ch.B.**[2], **Zhihong Wu**[1], and **Jiang Du, Ph.D.**[2]

[1]Department of Orthopedics, Peking Union Medical College, Beijing, China

[2]Department of Radiology, University of California, San Diego, CA

[3]Shiley Center for Orthopedic Research and Education at Scripps Clinic, La Jolla, CA

[#] These authors contributed equally to this work.

Abstract

Bone water exists in different states with the majority bound to the organic matrix and to mineral, and a smaller fraction in 'free' form in the pores of cortical bone. In this study we aimed to develop and evaluate ultrashort echo time (UTE) magnetic resonance imaging (MRI) techniques for assessment of T_2*, T_1 and concentration of collagen-bound and pore water in cortical bone using a 3T clinical whole-body scanner. UTE MRI together with an isotope study using tritiated and distilled water (THO-H_2O) exchange as well as gravimetrical analysis were performed on ten sectioned bovine bone samples. In addition, 32 human cortical bone samples were prepared for comparison between pore water concentration measured with UTE MRI and cortical porosity derived from micro computed tomography (μCT). A short T_2* of 0.27 ± 0.03 ms and T_1 of 116±6 ms were observed for collagen-bound water in bovine bone. A longer T_2* of 1.84 ± 0.52 ms and T_1 of 527±28 ms were observed for pore water in bovine bone. UTE MRI measurements showed a pore water concentration of 4.7-5.3% by volume and collagen-bound water concentration of 15.7-17.9% in bovine bone. THO-H_2O exchange studies showed a pore water concentration of 5.9 ± 0.6% and collagen-bound water concentration of 18.1 ± 2.1% in bovine bone. Gravimetrical analysis showed a pore water concentration of 6.3 ± 0.8% and collagen-bound water concentration of 19.2 ± 3.6% in bovine bone. A mineral water concentration of 9.5 ± 0.6% was derived in bovine bone with the THO-H_2O exchange study. UTE measured pore water concentration is highly correlated (R^2 = 0.72, P < 0.0001) with μCT porosity in the human cortical bone study. Both bovine and human bone studies suggest that UTE sequences could reliably measure collagen-bound and pore water concentration in cortical bone using a clinical scanner.

Keywords

bone; bound water; pore water; organic matrix; UTE

Corresponding Author: Jiang Du, Ph.D., jiangdu@ucsd.edu, University of California, San Diego, Department of Radiology, 200 West Arbor Drive, San Diego, CA 92103-8226, Phone (619) 471-0519, Fax (619) 471-0503.

Disclosures

All authors state that they have no conflicts of interest.

Introduction

Cortical bone is a composite material with three major components: mineral (principally hydroxyapatite, ~40% of bone by volume), collagen (~35% by volume) and water (~25% by volume) [1]. Dual-energy X-ray absorptiometry (DXA) and computed tomography (CT) have been used for quantitative analysis of bone mineral density (BMD) [2]. However, the organic matrix and water, which together represent ~60% of bone by volume, make little contribution to the signal obtained with these techniques. BMD measurement alone predicts fractures with only a 30-50% success rate [3,4]. From ages 60 to 80 years fracture risk increases about 13-fold, however the decrease in BMD alone only explains a doubling in this fracture risk [5]. A recent study of over 7800 patients reported that only 44% of all non-vertebral fractures occurred in women with a T-score below −2.5 (the World Health Organization definition of osteoporosis based on BMD), and this percentage dropped to 21% in men [6]. The limitations of BMD measurement have sparked research into the use of other imaging modalities to assess bone quality [7], focusing on architectural deterioration as well as the contribution of organic matrix and water to the biomechanical properties of cortical bone.

Water in cortical bone is present at various locations and in different states [8]. In normal bone a small fraction of water exists in ‘free’ form (pore water or PW) in Haversian canals (typical diameters ~50-200 μm) as well as in lacunae (~5 μm) and canaliculi (~0.1 μm) [9,10]. A larger portion of bone water exists in ‘bound’ form, either loosely bound to the organic matrix (collagen-bound water or CW) [11] or tightly bound to mineral (mineral-bound water or MW) [12,13]. Recent nuclear magnetic resonance (NMR) spectroscopy studies suggest that the loosely bound water concentration reflects organic matrix density of bone [14,15], while the “free” pore water concentration can potentially provide a surrogate measure of cortical porosity [16]. This provides an opportunity to develop noninvasive techniques to measure bound and pore water concentration in cortical bone and potentially provides a more accurate assessment of bone quality.

As a complementary tool to DXA and CT, magnetic resonance imaging (MRI) detects signal from protons (mostly water) in bone rather than from mineral. However, water in cortical bone has a very short apparent transverse relaxation time (or T_2*) and it provides no detectable signal when examined with conventional clinical MRI sequences [17]. Recently ultrashort echo time (UTE) sequences, with reduced nominal echo times (TEs) as short as 8 μs, which is about 100-1000 times shorter than the TEs of conventional clinical pulse sequences, have been used to detect signal from cortical bone [18]. More recently, magnetization prepared UTE techniques including adiabatic inversion recovery (AIR) and double adiabatic full passage (DAFP) sequences have been developed for mapping of bound and pore water in cortical bone in vivo [19]. This is important considering that bound and pore water make different contributions to the mechanical properties of cortical bone [20].

In this study we aimed to assess the value of two-dimensional (2D) and 3D UTE techniques for determining bound and pore water in bovine and human cortical bone samples. An isotope study, namely tritiated and distilled water (THO-H_2O) exchange in sectioned bovine bone samples, together with gravimetrical analysis were used to validate UTE-based cortical

bone water components quantification. A comparison study between UTE MRI measured pore water concentration and micro computed tomography (μCT) measured cortical porosity of cadaveric human cortical bone samples was also performed to further assess the accuracy of UTE MRI measurements of bone water components.

Materials and Methods

Sample Preparation

Fourteen bovine cortical bone samples of approximate dimensions 10×10×10 mm^3 were prepared from mature bovine femoral midshafts obtained from a local slaughterhouse. These samples were initially sectioned using a low-speed diamond saw (Isomet 1000, Buehler) with constant saline irrigation, and stored in phosphate buffered saline **(**PBS) solution for 24 hours prior to study. Four of the samples were used to determine the time required for THO and H_2O exchange to reach equilibrium. Ten samples were used for bound and pore water measurement with UTE and THO-H_2O isotope exchange studies (details below).

Cadaveric human cortical bone samples (n = 32) from 12 donors (7 females, 5 males, 30-92 years old) were obtained from tissue banks, as approved by Institutional Review Board. Using the precision circular diamond-edge saw and saline irrigation, larger bone blocks were sectioned into rectangular slabs of cortical bone with dimensions of ~1×1×10 mm^3. Individual samples were wrapped in saline-wet gauze and frozen at −70 °C in an ultralow freezer (Bio-Freezer; Forma Scientific, Marietta, OH, USA). The samples were allowed to thaw for 12 hours at 4 °C prior to UTE MR imaging and micro computed tomography (μCT).

Pulse Sequences

3D UTE sequences (Figure 1) were implemented on a 3T Signa TwinSpeed scanner (GE Healthcare Technologies, Milwaukee, WI). The basic 3D UTE sequence employed a short radio frequency (RF) rectangular pulse (duration = 26-52 μs) for signal excitation [21]. The z-gradient could be turned off to allow non-selective 2D UTE imaging for fast imaging of cortical bone. Both collagen-bound and pore water are detectable with the basic UTE sequences (Figure 1B). Furthermore, adiabatic inversion recovery prepared UTE (IR-UTE) sequences were developed for selective imaging of collagen bound water (Figure 1C). In the IR-UTE sequence, a Silver-Hoult adiabatic inversion pulse (duration = 8.64 ms, bandwidth = 1.5 kHz) was used to invert the longitudinal magnetization of pore water [18,22]. The longitudinal magnetization of collagen-bound water which has a very short T_2* was not inverted but largely saturated by the adiabatic IR pulse [22]. After an inversion time (TI) during which the inverted pore water magnetization approached the null point, the UTE acquisition was initiated to selectively detect signal from collagen-bound water (Figure 1D). 2D UTE and IR-UTE sequences were used for fast T1 and T2* quantification, while 3D UTE and IR-UTE sequences were used for bound and pore water concentration quantification (details below).

Quantitative MR Imaging

Collagen-Bound and Pore Water T_2*s—Each sample was placed in perfluorooctyl bromide (PFOB) solution. This helped maintain the hydration of cortical bone and minimize susceptibility effects at tissue-air interfaces. A birdcage coil (diameter = 2.5 cm, length = 12.2 cm) was used for signal excitation and reception. 2D UTE and IR-UTE sequences were performed for fast T_2* measurement with the following parameters: field of view (FOV) = 4 cm, sampling bandwidth (BW) = 62.5 kHz, flip angle = 10°, pulse duration = 26 μs, TR = 100 ms for UTE and 300 ms for IR-UTE, TI = 110 ms (for IR-UTE only), reconstruction matrix size = 128×128, in-plane pixel size = 0.31×0.31 mm^2, 211 projections, number of excitation (NEX) = 1, scan time = 21 sec for UTE and 1 min for IR-UTE. UTE and IR-UTE images were acquired at a series of TE delays (TE = 8 μs, 0.1, 0.2, 0.3, 0.4, 0.5, 0.6, 0.8, 1, 1.2, 1.4, 1.6, 2, 2.5, 3, 3.5, 4, 5, 6, 7 ms) to separate collagen-bound and pore water using the following bi-component analysis model [23]:

$$SI\,(t) = S_{z0,cw} \times e^{-t/T^*_{2,cw}} + S_{z0,pw} \times e^{-t/T^*_{2,pw}} + \text{noise} \quad [1]$$

where $S_{Z0,cw}$ and $S_{Z0,pw}$ are the magnetization of the collagen-bound and pore water components, and $T_{2,cw}$* and $T_{2,pw}$* are their T_2* relaxation times.

Collagen-Bound and Pore Water T_1s—Collagen-bound and pore water may have different T_1 values. Both contribute to the UTE signal when a minimal TE of 8 μs is used. When a longer TE (e.g., 2.4 ms) is used, the UTE signal mainly comes from pore water since the signal from collagen-bound water with a T_2* ~0.3 ms very largely decays to zero. In this study we proposed to use a saturation recovery dual echo UTE imaging technique to measure the T_{1s} of collagen-bound and pore water components.

In the saturation recovery UTE sequence a 90^0 rectangular pulse is followed by a crusher gradient to dephase signals from both long and short T_2 species. Dual echo 2D UTE acquisitions with progressively increasing saturation recovery times (TSRs) are used to detect the recovery of the longitudinal magnetization of cortical bone. For simplification, we assume an effective T_1 (T_1^{eff}) of collagen-bound and pore water is measured using 2D saturation recovery UTE acquisitions with a minimal TE of 8 μs, and pore water T_1 (T_1^{pw}) is measured using saturation recovery UTE acquisitions with a longer TE of 2.4 ms. T_1^{eff} and T_1^{pw} were calculated using the following two equations:

$$S\,(TSR, TE{=}8\mu s) = S_0 \times \left[1 - (1-k) \times e^{-TSR/T_1^{eff}}\right] + C \quad [2]$$

$$S\,(TSR, TE{=}2.4ms) = S_0 \times \left[1 - (1-k) \times e^{-TSR/T_1^{pw}}\right] + C \quad [3]$$

where k accounts for the residual fraction of the longitudinal magnetization of cortical bone after a nominal 90° pulse. Similar imaging parameters were used except for a long TR of

3500 ms (which is long enough to ensure almost complete recovery of both bound and pore water longitudinal magnetizations after each 90° pulse), TE = 8 μs and 2.4 ms, a series of TSRs (7, 25, 50, 100, 200, 400, 600, 800, 1000, 1200, 1600, 2000, 2400, 2800, 3400 ms) with a total scan time of 110 min.

The collagen-bound water signal obtained with IR-UTE imaging can be described by the following equation [24]:

$$S_{IR-UTE}\left(TR,TI,TE{=}8\mu s\right) \propto \frac{\left[1-(1-Q)\times e^{-TI/T_1^{CW}}-Q\times e^{-TR/T_1^{CW}}\right]}{1-Q\times cos\left(\theta\right)\times e^{-TR/T_1^{CW}}}\times sin\left(\theta\right)\times e^{-TE/T_{2,cw}^{*}} \quad [4]$$

where T_1^{CW} is the T_1 of collagen-bound water, and Q is the inversion efficiency of the adiabatic IR pulse. For collagen-bound water with a T_2* of ~0.3 ms, Q approximates 0 (i.e., < 0.04) according to Bloch equation simulation [18]. As a result, the IR-UTE signal can be simplified as follows [24]:

$$S_{IR-UTE} \propto 1-e^{-TI/T_1^{CW}} \quad [5]$$

here T_1^{CW} can be measured by fitting the IR-UTE signal acquired with a series of TR and TI combinations, under the condition that each TR/TI combination satisfies the inversion and nulling condition necessary to suppress the signal from pore water. We used imaging parameters similar to the 2D IR-UTE T_2* analysis above, but with a series of TR/TI combinations (e.g., TR = 50, 100, 200, 300, 400, 500 ms, TI was chosen for each sample based on the criteria to null pore water with a measured T_1^{pw}). The total scan time was about 6 min.

Collagen-Bound and Pore Water Concentration Measurement—Total water concentration (WC_{Total}) was measured by comparing the 3D UTE signal intensity of cortical bone with that from a doped water phantom [25]. Accurate estimation of bone water requires consideration of relaxation times and coil sensitivity. In our experiments the external reference was a mixture of distilled water (20%) and D_2O (80%) doped with 26 millimolar $MnCl_2$, resulting in a short T_2* of ~300 μs and a T_1 of ~ 5 ms (measured with standard UTE acquisitions wit variable TEs or TSRs, as shown in Ref 18). With the use of a short excitation pulse (14 μs), ultrashort TE (8 μs), relatively long TR (50 ms) and a small flip angle (5°), T_1 and T_2* relaxation effects can be ignored, and WC_{Total}^{UTE} can be simplified as follows:

$$WC_{Total}^{UTE} \approx \frac{I_{bone}^{UTE}}{I_{H_2O-D_2O}^{UTE}}\times\eta\times 20\% \quad [6]$$

where I_{bone}^{UTE} and $I_{H_2O-D_2O}^{UTE}$ are the 3D UTE signal intensities of cortical bone and H_2O-D_2O water phantom, respectively, and η is a coil sensitivity correction. η was corrected by dividing the 3D UTE signal from cortical bone or doped water phantom by the 3D UTE signal obtained from a separate scan of a bottle of water, which was large enough to cover the region occupied by both the cortical bone sample and doped water phantom. Other imaging parameters were similar to those used for 2D UTE T_2* measurements except for 3D UTE acquisitions with 20,000 projections and a voxel size of 0.31×0.31×0.31 mm^3. The total scan time was 16.7 min.

Collagen-bound water concentration ($WC_{Collagen}$) was measured by comparing the 3D IR-UTE signal intensity of cortical bone with that from the water phantom. Based on Eq.4, $WC_{Collagen}^{IR-UTE}$ can be measured as follows:

$$WC_{Collagen}^{IR-UTE} \approx \frac{1-e^{-TI/T_1^{H_2O-D_2O}}}{1-e^{-TI/T_1^{CW}}} \times \frac{I_{bone}^{IR-UTE}}{I_{H_2O-D_2O}^{IR-UTE}} \times \eta \times 20\% \approx \frac{I_{bone}^{IR-UTE}}{I_{H_2O-D_2O}^{IR-UTE} \times \left(1-e^{-TI/T_1^{CW}}\right)} \times \eta \times 20\% \quad [7]$$

where I_{bone}^{IR-UTE} and $I_{H_2O-D_2O}^{IR-UTE}$ are the IR-UTE signal intensities of cortical bone and H_2O-D_2O water phantom, respectively. After each IR pulse the longitudinal magnetization of H_2O-D_2O is almost fully recovered since its T_1 is much shorter than TI. Imaging parameters were similar to those used for 2D IR-UTE T_2* measurements, except for 3D IR-UTE with 20,000 projections and a voxel size of 0.31×0.31×0.31 mm^3. The total scan time was 100 min.

With total water and collagen-bound water known, pore water concentration (WC_{Pore}) can be calculated as their difference:

$$WC_{Pore} = WC_{Total}^{UTE} - WC_{Collagen}^{IR-UTE} \quad [8]$$

μCT Imaging—The human cortical bone samples were imaged using a μCT scanner (1076, Skyscan, Kontich, Belgium) with the following parameters: 0.5 mm Aluminum filter, 72 kV, 140 μA, 720 views collected at 0.5° increments corresponding to one full rotation of each bone specimen, FOV 25 mm, isotropic 9 μm voxels. The total scan time was ~ 3 hours.

THO-H_2O exchange study—THO is radioactive, with a half life of 12.3 years. The relatively long half life makes it ideal for isotope study. Four bovine cortical samples were used to determine the time required for THO-H_2O exchange to reach equilibrium. Each bone sample was blotted dry and put in a glass bottle filled with 2 ml of THO for times of 1, 2, 4, 7 and 10 days and maintained at room temperature. After each exchange stage, 0.1 ml of the mixed solution (a mixture of THO and H_2O) was mixed by vortex with 5 ml of scintillation

fluid (Ecoscint, National Diagnostics, Atlanta, GA) in scintillation vials and placed into a liquid scintillation counter (LS6000SC, Beckman Coulter Inc, Brea, CA) for beta radiation measurement in counts per minute (CPM). CPM is defined by the total number of photons counted divided by the count time. CPM was plotted against isotope exchange time to determine the time required to reach equilibrium.

Each glass vial containing an individual bone sample was filled with 2 ml of THO. The glass vial was tightly sealed for THO-H_2O exchange. After equilibrium (~7 days) 0.1 ml of the mixed solution was prepared for beta radiation detection. Meanwhile a calibration curve was generated by measuring the radiation of solutions with eight different ratios (1:0, 1:0.05, 1:0.1, 1:0.15, 1:0.2, 1:0.3, 1:0.5 and 1:1) of THO and H_2O. CPM was plotted against the THO dilution factor and then used as the calibration curve. Based on the radiation calibration curve a dilution factor for the THO-H_2O exchange was calculated, and used for accurate measurement of the volume of H_2O in each bovine cortical bone. Bone water concentration was calculated by dividing H_2O volume by bone volume from μCT (more details are given in the Gravimetrical Analysis section below).

Gravimetrical Analysis—Previous literatures suggest that air-drying at room temperature mainly results in loss of pore water, while subsequent oven-drying at 60-100 °C mainly results in loss of water bound to the organic matrix [26–30]. In this study we employed air-drying (in an oven with controlled humidity at room temperature) of blot-dried bovine cortical bone for 48 hours to remove pore water, followed by oven-drying at 100 °C for 72 hours to remove collagen-bound water, after which water remaining in the bone is assumed to be tightly bound to mineral. The air-drying and oven-drying times were empirically determined based on weight change. About two days were needed for air-drying and three days were needed for oven-drying to reach equilibrium mass (weight change of less than 0.1% in the last five hours of drying).

Mankin et al. used an approach combining THO-H_2O exchange and drying course to measure bound and free water in articular cartilage [31]. We adopted a similar approach in this study. First, all bovine cortical bone samples (n=10) were blotted dry and subjected to UTE and IR-UTE imaging to quantify T_1^{pw}, T_1^{cw}, $T_{2,pw}$*, $T_{2,cw}$*, $WC_{Collagen}$ and WC_{Pore}, and μCT imaging to measure bone volume ($V_{bone}^{bolt-dry}$), as well as use of a digital precision balance (Mettler Toledo AL104) to measure bone weight ($W_{bone}^{bolt-dry}$). Then half of the bone samples (n=5) were subjected to air-drying to remove pore water, followed by measurement of bone weight ($W_{bone}^{air-dry}$). The volume of H_2O from each blot-dried ($V_{water}^{blot-dry}$) and air-dried ($V_{water}^{air-dry}$) bovine cortical bone sample was measured via THO-H_2O exchange. Each bone sample was then immersed in saline (50 ml), changed daily until the CPM was reduced to background level (<40), indicating that all THO had been replaced by H_2O. Oven-drying for 72 hours at 100 °C was used to remove collagen-bound and pore water. Each bovine bone sample was cooled down in a sealed glass tube to minimize reabsorbtion of water. The oven-dry weight was measured as $W_{bone}^{oven-dry}$. Finally each bone sample was placed into THO-H_2O for a second THO-H_2O exchange to measure the volume of mineral-bound water ($V_{water}^{oven-dry}$) which had not been removed by the oven-drying process. Total bone water

concentration from the THO-H_2O exchange study ($WC_{Total}^{THO-H_2O}$) was calculated as follows:

$$WC_{Total}^{THO-H_2O} \approx \frac{V_{water}^{blot-dry}}{V_{bone}^{blot-dry}} \times 100\% \quad [9]$$

The concentration of water bound to collagen ($WC_{Collagen}^{THO-H_2O}$) was calculated as follows:

$$WC_{Collagen}^{THO-H_2O} \approx \frac{V_{water}^{air-dry} - V_{water}^{oven-dry}}{V_{bone}^{blot-dry}} \times 100\% \quad [10]$$

The concentration of water bound to mineral ($WC_{Mineral}^{THO-H_2O}$) was calculated as follows:

$$WC_{Mineral}^{THO-H_2O} \approx \frac{V_{water}^{oven-dry}}{V_{bone}^{blot-dry}} \times 100\% \quad [11]$$

Pore water concentration ($WC_{Pore}^{THO-H_2O}$) was calculated as follows:

$$WC_{Pore}^{THO-H_2O} = WC_{Total}^{THO-H_2O} - WC_{Collagen}^{THO-H_2O} - WC_{Mineral}^{THO-H_2O} \quad [12]$$

Both pore water ($WC_{Pore}^{Gravimetry}$) and collagen-bound water ($WC_{Collagen}^{Gravimetry}$) can also be estimated from the gravimetric measurements using the following equations [29]:

$$WC_{Pore}^{Gravimetry} \approx \frac{W_{water}^{blot-dry} - W_{water}^{air-dry}}{V_{bone}^{blot-dry}} \times 100\% \quad [13]$$

$$WC_{Collagen}^{Gravimetry} \approx \frac{W_{water}^{air-dry} - W_{water}^{oven-dry}}{V_{bone}^{blot-dry}} \times 100\% \quad [14]$$

Mineral-bound water is inaccessible with gravimetric analysis due to the difficulty in separating it from collagen gravimetrically.

Data Analysis

A semi-automated MATLAB (The Mathworks Inc. Natick, MA, USA) program was developed for single- and bi-component T_2* and T_1 analysis. Regions of interest (ROIs) were drawn in the central part of cortical bone for data analysis. Goodness of fit statistics

including the R-squared value and standard error or fitting confidence level were computed. Fit curves along with their 95% confidence intervals (CI) and residual signal curves were created. Total, collagen-bound, mineral-bound and pore water concentrations were calculated using the equations shown in [6-14].

For each human cortical bone sample, 12 μCT images every 2.5 mm along the sample long axis were selected and imported into Matlab. A custom program was used to determine the global histogram for all the images and this was used to determine a local minimum value used for thresholding. Binarized images were despeckled to remove noise, and regions of interest corresponding to the outer boundary of the sample as well as to bone were automatically generated. Cortical porosity was determined as one minus the ratio of the area of the bone to that of the outer boundary of the sample.

Results

UTE and IR-UTE sequences were used to access different water components in cortical bone using a clinical MR scanner. Figure 2 shows selected UTE and IR-UTE images of a bovine cortical bone sample with different TEs. Systematic residual signal is seen with single-component fitting of UTE signal decay, suggesting the existence of another water component. Excellent curve fitting is achieved with a bi-component model which shows two distinct water components: one with a short T_2* of 0.26 ms accounting for 72.4% of the total UTE signal, and the other with a longer T_2* of 1.56 ms accounting for 27.6% of the signal decay. The shorter and longer T_2* values are consistent with those of collagen-bound and pore water respectively based on recent NMR spectroscopic studies by Ni et al., who reported a short T2* of 0.21 ms and a longer T2* of 2.70 ms [16], suggesting that UTE bi-component analysis can access bound and pore water using a whole-body clinical MR scanner. The IR-UTE images show a single component T_2* decay of 0.31 ms which is close to the short T_2* value of 0.26 ms obtained from the bi-component fitting of UTE T_2* signal decay, suggesting that water bound to the organic matrix is selectively detected in IR-UTE imaging. The pore water component with a longer T_2* is largely suppressed by the IR preparation pulse through adiabatic inversion and signal nulling.

Table 1 shows the mean and standard deviation of T_2* values of 10 bovine bone samples. An effective T_2* of 0.41 ± 0.05 ms was demonstrated from single-component fitting of UTE signal decays with contribution from both collagen-bound and pore water components. Bi-component fitting shows a mean pore water T_2^{*pw} of 0.28 ± 0.03 ms and collagen-bound water T_2^{*cw} of 1.84 ± 0.52 ms, with a fraction of 25.4 ± 4.2% and 74.6 ± 4.2%, respectively. The IR-UTE signal shows an excellent single-component decay behavior, with a mean T_2^{*cw} of 0.32 ± 0.02 ms, which is comparable to that derived from bi-component fitting of UTE signal decay.

Figure 3 shows T_1 measurements using saturation recovery dual echo UTE acquisitions as well as IR-UTE acquisitions with variable TR/TI combinations. Single-component fitting of the saturation recovery curve shows a T_1^{eff} of 268 ms, which is the effective T_1 of collagen-bound and pore water since both water components contribute to the UTE signal with a minimal TE of 8 μs, and a T_1^{pw} of 509 ms, which is the T_1 of pore water only since signal

from collagen-bound water decays to near zero with a TE of 2.4 ms. Exponential fitting of the IR-UTE curve shows a T_1^{cw} of 122 ms, which is likely the T_1 of collagen-bound water since signal from pore water is selectively suppressed with each of IR-UTE acquisitions with variable TR/TI combinations.

Table 2 shows the mean and standard deviation of T_1 values of 10 bovine bone samples. A mean effective T_1^{eff} of 243 ± 37 ms was demonstrated from single-component fitting of saturation recovery UTE signal recovery with a TE of 8 μs, where both collagen-bound and pore water components contributed to the UTE signal recovery. A mean pore water T_1^{pw} of 527 ± 28 ms was demonstrated from single-component fitting of saturation recovery UTE signal recovery with a TE of 2.4 ms, where only pore water contributed to the UTE signal recovery. A mean collagen-bound water T_1^{cw} of 116 ± 6 ms was demonstrated from single-component fitting of IR-UTE signal recovery with different TR/TI combinations. T_1^{cw} is significantly shorter than T_1^{pw}.

Measurement of bone water concentration using THO-H_2O isotope exchange requires calibration. Figure 4 shows the calibration curves generated for water concentration measurement in the THO-H_2O experiment. An excellent linear relationship ($R^2 = 0.9997$) between CPM and THO fractions in THO-H_2O solutions was observed, suggesting that dilution factor, and thus water concentration from bovine cortical bone can be accurately measured by linearly interpolating CPM of the THO-H_2O mixed solution.

Total, bound and pore water concentration in bovine cortical bone measured with UTE MRI, THO-H_2O isotope exchange and gravimetrical analysis are shown in Table 1. UTE measured collagen-bound and pore water concentration approximates that determined by THO-H_2O isotope exchange and gravimetrical analysis, suggesting that UTE sequences can reliably measure collagen-bound and pore water in cortical bone. Furthermore, THO-H_2O study of oven-dried bone suggests the existence of a significant portion of bone water (~9.5% by volume), which is likely to be water tightly bound to mineral that has not been identified previously.

A high correlation ($R^2 = 0.72$; $P < 0.0001$) was observed between μCT porosity and pore water concentration in 32 cadaveric human cortical bone samples, as shown in Figure 5. Water residing in the microscopic pores of cortical bone is expected to behave more like ‘free’ water. The high correlation between μCT porosity and ‘free’ water concentration further confirmed the accuracy of UTE techniques in assessing bound and ‘free’ water in cortical bone. μCT porosity is consistently lower that ‘free’ water content assessed by UTE MRI, likely due to “free” water in smaller pores being detected by UTE MRI but not μCT imaging.

Discussion

UTE imaging has the potential to assess different water components in cortical bone in vivo. Our data indicates that UTE sequences detect both collagen-bound and pore water in cortical bone when using a clinical whole-body 3T scanner. The excellent bi-component fitting suggests that no more than two components are needed to explain the UTE signal decay

behavior. The majority of the bone water (70-80%) exists in the form of collagen-bound water in cortical bone. The IR-UTE signal decay shows excellent single-component decay behavior with an untrashort T_2* of around 0.3 ms, suggesting that only collagen-bound water is detected by the IR-UTE sequence with pore water effectively suppressed by the adiabatic IR pulse. UTE measured pore water is about 10~20% lower than that measured with THO-H_2O isotope exchange, and 15~25% lower than that measured with gravimetric analysis, partly because of the loss of loosely bound water during air-drying at room temperature [26-29]. Furthermore, air-drying may not fully remove all pore water, further complicating the comparisons [26]. The high correlation (R^2 = 0.72) between UTE measured pore water concentration and μCT cortical porosity further suggests that UTE and IR-UTE sequences can reliably access total and collagen-bound water components in cortical bone.

Previous NMR spectroscopy studies have confirmed the existence of multiple water components in cortical bone. Proton NMR spin grouping and exchange in dentin, a bone-like hard tissue, shows that 30% of the water is strongly bound to mineral with a T_2* of ~ 12 μs, 52% of the water is loosely bound to the organic matrix with a T_2* of ~200 μs, and 18% of the water is trapped in the dentinal tubules with a T_2* of ~1000 μs [12]. Considering that mineral-bound water has a too short T_2* to be detected by clinical MR scanners, loosely bound water accounts for ~75% of the total UTE detectable signal. Inversion relaxation analysis of FID signal of bone samples also showed three distinct signal components with T_2*s of ~11μs, ~210 μs, and ~2.7 ms, respectively [16]. Multiple component analysis of FID and CPMG signals of cortical bone samples identified five signal sources, including collagen-bound water, pore water, mineral-bound water, collagen methylene, and lipid methylene [11]. Mineral-bound water has an extremely short T_2* of ~11.8 μs, accounting for ~8% of total water in bone. Collagen-bound water accounts for ~73% of total water, with the other ~18% for pore water. Furthermore, our measured mean T_1^{pw} of 527 ± 28 ms for bovine cortical bone samples at 3T are comparable with the recent published results by Horch, et al [22], who reported a mean T_1^{pw} of 551 ± 120 ms for human cortical bone samples at 4.7 T. Our measured mean T_1^{cw} of 116 ± 6 ms at 3 T is significantly shorter than the mean T_1^{cw} of 357 ± 10 ms at 4.7 T reported by Horch et al [22]. This might be partly due to the field dependence of T_1. More recently Seifert et al reported a mean T_1^{pw} of 880 ± 281 ms and a mean T_1^{cw} of 145 ± 25 ms at 3 T[28]. T_1^{cw} value from our study is very close to that reported by Seifert et al [28]. Meanwhile, the mean T_1^{pw} values of 880 ± 281 ms at 3T and 1790 ± 470 ms at 7T from the Seifert study are significantly higher than the mean T_1^{pw} values of 527 ± 28 ms at 3T from our study and 551 ± 120 ms at 4.7T from the Horch study [22, 28]. The difference might be due to multiple factors, including different field strengths (T_1 is field strength dependent) and type of specimen (T_1^{pw} in human cortical bone with bigger pores is expected to be longer than in bovine cortical bone with smaller pores).

Bulk water in the pores has a long T_2 (> 100 ms) but a short T_2* (< 10 ms), and can be detected with conventional clinical fast spin echo (FSE) sequences with TEs of 10 ms or longer [32]. FSE-determined porosity is highly correlated (R^2 = 0.83) with μCT porosity [33]. However, it should be noted that not all “free” water in pores has T2* long enough to be detectable by conventional FSE sequences. There is a broad distribution of T2 and T2* values in pore water [11, 30]. Water loosely bound to the organic matrix has very short T_2 and T_2*, and remains invisible to conventional clinical MR sequences. Wu et al developed water-

and fat-suppressed proton projection MRI (WASPI) for bone imaging in vitro [15]. Gravimetric and amino analyses showed that the WASPI signal is highly correlated (R^2 = 0.98) with collagen content [14]. Water tightly bound to mineral has an extremely short T_2*. Bone mineral crystals contain hydroxyl (OH^-) ions which can be observed with proton magic angle spinning (MAS) NMR spectroscopy [34]. More recently, using the 2D Lee-Goldberg cross-polarization under magic-angle spinning (2D LG-CPMSA) pulse sequence, Wilson et al observed a structured water layer at the surface of the mineral in cortical bone [35]. In a later study, they identified three types of structurally-bound water [36], which serves to stabilize these defect-containing crystals or mediating mineral-organic matrix interactions. Tightly-bound water was also observed by Ivanova et al. using proton MAS NMR spectroscopy [37]. However, water bound to mineral is largely neglected in commonly used drying techniques [26–29]. The difference between oven-dried weight and ash weight is typically considered to be the weight of the organic phase [29]. This simplification is expected to overestimate the organic matrix content, and underestimate the total water content in cortical bone. As our study indicated, approximately 28% of bone water (i.e., mineral-bound water) would be misclassified as organic matrix content according to the conventional gravimetric techniques.

The strength of bone is determined by its composition and structure. Recent work by Zebaze et al. suggested that accurate assessment of bone structure, especially cortical porosity, could improve identification of individuals at high risk of fracture and assist treatment [38]. Age related adverse changes in the collagen network may lead to the decreased toughness of bone [39]. A recent work done by Gallant et al. [40] found that collagen-bound water, rather than pore water, was highly correlated with canine bone biomechanics following raloxifene treatment, while cortical porosity, BMD and bone mineral concentration (BMC) show no significant correlation. Those results suggest the importance of simultaneous assessment of bound and pore water in cortical bone. More recently, two other UTE-derived indices, the porosity index [41] and suppression ratio [42], were introduced. However, these indices only indirectly measure bone quality without direct information on cortical porosity and collagen content. The 3D UTE and IR-UTE techniques introduced in this study have the potential to assess organic matrix via bound water measurement and cortical porosity via pore water measurement, thus allowing direct comparison of cortical porosity and collagen matrix across different groups of people (e.g., aging and disease related changes in cortical bone). UTE together with magnetization transfer (MT) imaging may provide further information on mineral-bound water, and potentially bone mineral content [43]. More importantly, these techniques allow accurate volumetric mapping of different water components in cortical bone in vivo in a time-efficient way using clinical whole-body scanners. This may significantly advance the study of bone diseases including OP, osteomalacia, osteopenia, Paget disease, renal osteodystrophy and insufficiency fractures in the setting of biophosphonate therapy or raloxifene treatment [40].

There are several limitations in this study. First, the 2D and 3D UTE sequences are time consuming, limiting their clinical applications. However, more advanced UTE sequences employing a 3D Cones trajectory have shown promise in measuring bound and pore water in cortical bone in vivo [44]. Second, the 2D and 3D UTE sequences are based on the use of T_2* than T_2 to separate bound water from pore water. Susceptibility and surface relaxation

shortening of the pore water components, making it challenging to achieve robust separation of bound water and pore water especially at higher field strengths [28]. Third, reference techniques including THO-H_2O isotope exchange and gravimetrical method have limitations [26,29]. During air-drying bound water is partly removed. Oven-drying cannot completely remove all the bound water, especially water tightly bound to bone mineral. T_2 spectral analysis is a more accurate technique in separating bound and pore water [28]. However, it is technically difficult or impossible to acquire multi-echo spin echo data for T_2 analysis in vivo, due to the limitations in RF power and specific absorption ratio (SAR) associated with clinical MR scanners. Fourth, no comparison has been done between our 2D and 3D UTE techniques and several other short T_2 imaging techniques, such as zero echo time (ZTE) imaging [45], pointwise encoding time reduction with radial acquisition (PETRA) [46], double adiabatic full passage (DAFP) [19], and sweep imaging with Fourier transformation (SWIFT) [47]. Imaging techniques such as ZTE and SWIFT have potential advantages over 2D and 3D radial UTE sequences when imaging extremely short T2 species due to their shorter effective TEs. However, the contrast mechanisms associated with ZTE and SWIFT, and their applications in measuring bound and pore water T_1s, T_2*s and water concentrations remain to be established. Fifth, computed tomography (CT) is an established imaging technique for studying bone mineral density and content. Comparison between UTE MRI and CT techniques would be of considerable interest and will be performed in future studies.

In conclusion, we have demonstrated that T_1, T_2* and concentration of collagen-bound and pore water components can be measured with UTE and IR-UTE sequences. Further clinical studies will be necessary to evaluate the diagnostic power of this method.

Acknowledgement

The authors acknowledge grant support from GE Healthcare, Donald and Darlene Shiley, and NIH (1R01 AR062581-01A1 and 1R21 AR063894-01A1).

Abbreviations used

2D	two-dimensional
BMC	bone mineral concentration
BMD	bone mineral density
CPM	counts per minute
CW	collagen-bound water
DXA	Dual-energy X-ray absorptiometry
FSE	fast spin echo
FID	free induction decay
FOV	field of view

IR	inversion recovery
LG-CPMSA	Lee-Goldberg cross-polarization under magic-angle spinning
MAS	magic angle spinning
MRI	magnetic resonance imaging
MT	magnetization transfer
NEX	number of excitations
NMR	nuclear magnetic resonance
PFOB	perfluorooctyl bromide
PBS	phosphate buffered saline
PW	pore water
RF	radio frequency
ROI	region of interest
SNR	signal to noise ratio
TE	echo time
TI	inversion time
TSR	saturation recovery time
μCT	micro computed tomography
UCSD	University of California, San Diego
UTE	ultrashort echo time
WASP	water- and fat-suppressed proton projection MRI

References

1. American Society for Bone and Mineral Research ASBMR. Bone Curriculum. 2004. http://depts.washington.edu/bonebio/ASBMRed/ASBMRed.html
2. Kalpakcioglu BB, Morshed S, Engelke K, Genant HK. Advanced imaging of bone macrostructure and microstructure in bone fragility and fracture repair. J Bone Joint Surg Am. 2008; 90:68–78. [PubMed: 18292360]
3. Kanis JA, Johnell O, Oden A, Dawson A, De Laet C, Jonsson B. Ten year probabilities of osteoporotic fractures according to BMD and diagnostic thresholds. Osteoporos Int. 2001; 12:989–995. [PubMed: 11846333]
4. Faulkner KG. Bone matters: are density increases necessary to reduce fracture risk? J Bone Miner Res. 2000; 15:183–187. [PubMed: 10703919]
5. De Lact C, van Hout B, Burger H, Hofman A, Pols H. Bone density and the risk of hip fracture in men and women: cross sectional analysis. Br Med J. 1997; 315:221–225. [PubMed: 9253270]

6. Schuit SCE, Klift M, Weel AEAM, Laet CEDH de, Burger H, Seeman E, Hofman A, Uitterlinden AG, Leeuwen JPTM van, Pols HAP. Fracture incidence and association with bone mineral density in elderly men and women: the Rotterdam study. Bone. 2004; 34:195–202. [PubMed: 14751578]
7. Link TM. The Founder's Lecture 2009: advances in imaging of osteoporosis and osteoarthritis. Skeletal Radiol. 2010; 39:943–955. [PubMed: 20563801]
8. Wehrli FW, Song HK, Saha PK, Wright AC. Quantitative MRI for the assessment of bone structure and function. NMR in Biomed. 2006; 19:731–764.
9. Seeman E, Delmas PD. Bone quality – the material and structural basis of bone strength and fragility. N Engl J Med. 2006; 354:2250–2261. [PubMed: 16723616]
10. Cowin SC. Bone poroelasticity. J Biomechanics. 1999; 32:217–238.
11. Horch RA, Nyman JS, Gochberg DF, Dortch RD, Does MD. Characterization of 1H NMR signal in human cortical bone for magnetization resonance imaging. Magn Reson Med. 2010; 64:680–687. [PubMed: 20806375]
12. Schreiner LJ, Cameron IG, Funduk N, Miljkovic L, Pintar NN, Kydon DN. Proton NMR spin grouping and exchange in dentin. Biophys J. 1991; 59:629–639. [PubMed: 2049523]
13. Cho G, Wu Y, Ackerman JL. Detection of hydroxyl ions in bone mineral by solid-state NMR spectroscopy. Science. 2003; 300:1123–1127. [PubMed: 12750514]
14. Cao H, Ackerman JL, Hrovat MI, Graham L, Glimcher MJ, Wu Y. Quantitative bone matrix density measurement by water- and fat-suppressed proton projection MRI (WASPI) with polymer calibration phantoms. Magn Reson Med. 2008; 60:1433–1443. [PubMed: 19025909]
15. Wu Y, Chesler DA, Glimcher MJ, Garrido L, Wang J, Jiang HJ, Ackerman JA. Multinuclear solid-state three-dimensional MRI of bone and synthetic calcium phosphates. Proc Natl Acad Sci. 1999; 96:1574–1578. [PubMed: 9990066]
16. Ni Q, Nyman JS, Wang X, Santos ADL, Nicolella DP. Assessment of water distribution changes in human corticalbone by nuclear magnetic resonance. Meas Sci Technol. 2007; 18:715–723.
17. Robson MD, Gatehouse PD, Bydder M, Bydder GM. Magnetic resonance: an introduction to Ultrashort TE (UTE) imaging. J Comput Assist Tomogr. 2003; 27:825–846. [PubMed: 14600447]
18. Du J, Carl M, Bydder M, Takahashi A, Chung CB, Bydder GM. Qualitative and quantitative ultrashort echo time (UTE) imaging of cortical bone. J Magn Reson. 2010; 207:304–311. [PubMed: 20980179]
19. Manhard MK, Horch RA, Gochberg DF, Nyman JS, Does MD. In vivo quantitative MR imaging of bound and pore water in cortical bone. Radiology. May.2015 25:140336.
20. Horch RA, Gochberg DF, Nyman JS, Does MD. Non-invasive Predictors of Human Cortical Bone Mechanical Properties: T-2-Discriminated H-1 NMR Compared with High Resolution X-ray. PLoS ONE. 2011; 6(1):e16359. [PubMed: 21283693]
21. Du J, Bydder M, Takahashi AM, Carl M, Chung CB, Bydder GM. Short T2 contrast with three-dimensional ultrashort echo time imaging. Magn Reson Imaging. 2011; 29:470–82. [PubMed: 21440400]
22. Horch R, Gochberg D, Nyman J, Does M. Clinically-compatible MRI strategies for discriminating bound and pore water in cortical bone. Magn Reson Med. 2012; 68:1774–1784. [PubMed: 22294340]
23. Diaz E, Chung CB, Bae WC, Statum S, Znamirowski R, Bydder GM, Du J. Ultrashort echo time spectroscopic imaging (UTESI): an efficient method for quantifying bound and free water. NMR in Biomed. 2012; 25:161–8.
24. Du J, Sheth V, He Q, Carl M, Chen J, Corey-Bloom J, Bydder GM. Measurement of T1 of the ultrashort T2* components in white matter of the brain at 3T. PLOS One. 2014; 9(8):e103296. [PubMed: 25093859]
25. Techawiboonwong A, Song HK, Leonard MB, Wehrli FW. Cortical bone water: in vivo quantification with ultrashort echo-time MR imaging. Radiology. 2008; 248:824–833. [PubMed: 18632530]
26. Nyman JS, Roy A, Shen X, Rae LA, Tyler JH, Wang X. The influence of water removal on the strength and toughness of cortical bone. J Biochem. 2006; 39:931–938.

27. Biswas R, Bae CW, Diaz E, Masuda K, Chung CB, Bydder GM, Du J. Ultrashort echo time (UTE) imaging with bi-component analysis: bound and free water evaluation of bovine cortical bone subject to sequential drying. Bone. 2012; 50:749–755. [PubMed: 22178540]
28. Seifert AC, Wehrli SL, Wehrli FW. Bi-component T2* analysis of bound and pore bone water fractions fails at high field strengths. NMR Biomed. 2015; 28:861–872. [PubMed: 25981785]
29. Yeni YN, Brown CU, Norman TL. Influence of bone composition and apparent density on fracture toughness of the human femur and tibia. Bone. 1998; 22:79–84. [PubMed: 9437517]
30. Nyman JS, Ni Q, Nicolella DP, Wang X. Measurements of mobile and bound water by nuclear magnetic resonance correlate with mechanical properties of bone. Bone. 2008; 42:193–199. [PubMed: 17964874]
31. Mankin HJ, Thrasher AZ. Water content and binding in normal and osteoarthritic human cartilage. J Bone Joint Surg. 1975; 57:76–80. [PubMed: 1123375]
32. Du J, Hermida JC, Diaz E, Corbeil J, Znamirowski R, D'Lima DD, Bydder GM. Assessment of cortical bone with clinical and ultrashort echo time sequences. Magn Reson Med. 2013; 70:697–704. [PubMed: 23001864]
33. Bae WC, Patil S, Biswas R, Li S, Chang EY, Statum S, Dlima DD, Chung CB, Du J. Magnetic resonance imaging assessed cortical porosity is highly correlated with μCT porosity. Bone. 2014; 66:56–61. [PubMed: 24928498]
34. Yesinowski JP, Eckert H. Hydrogen environments in calcium phosphates: proton MAS NMR at high spinning speeds. J Am Chem Soc. 1987; 109:6274–6282.
35. Wilson EE, Awonusi A, Morris MD, Kohn DH, Tecklenburg M, Beck LW. Highly ordered interstitial water observed in bone by nuclear magnetic resonance. J Bone Miner Res. 2005; 20:625–634. [PubMed: 15765182]
36. Wilson EE, Awonusi A, Morris MD, Kohn DH, Tecklenburg M, Beck LW. Three structural roles for water in bone observed by solid-state NMR. Biophys J. 2006; 90:3722–3731. [PubMed: 16500963]
37. Ivanova TI, Frank-Kamenetskaya OV, Kol'tsov AB, Ugolkov VL. Crystal structure of calcium-deficient carbonate hydroxyapatite. Thermal decomposition. J Solid State Chem. 2001; 160:340–349.
38. Zabaze RMD, Ghasem-Zadeh A, Bohte A, Luliano-Burns S, Mirams M, Price RI, Mackie EJ, Seeman E. Intracortical remodeling and porosity in the distal radius and post-mortem femurs of women: a cross-sectional study. Lancet. 2010; 375:1729–1736. [PubMed: 20472174]
39. Wang X, Li SX, Mauli Agrawal C. Age-related changes in the collagen network and toughness of bone. Bone. 2002; 31:1–7. [PubMed: 12110404]
40. Gallant MA, Brown DM, Hammond M, Wallace JM, Du J, Deymier-Black AC, Almer JD, Stock SR, Allen MR, Burr DB. Bone cell-independent benefits of raloxifene on the skeleton: a novel mechanism for improving bone material properties. Bone. 2014; 61:191–200. [PubMed: 24468719]
41. Rajapakse CS, Bashoor-Zadeh M, Li C, Sun W, Wright AC, Wehrli FW. Volumetric cortical bone porosity assessment with MR imaging: validation and clinical feasibility. Radiology. May.2015 19:141850.
42. Li C, Seifert AC, Rad HS, Bhagat Y, Rajapakse CS, Sun W, Benny Lam SC, Wehrli FW. Cortical Bone Water Concentration: Dependence of MR Imaging Measures on Age and Pore Volume Fraction. Radiology. 2014; 272:796–806. [PubMed: 24814179]
43. Springer F, Martirosian P, Machann J, Schwenzer NF, Claussen CD, Schick F. Magnetization transfer contrast imaging in bovine and human cortical bone applying an ultrashort echo time sequence at 3 Tesla. Magn Reson Med. 2009; 61:1040–8. [PubMed: 19267348]
44. Carl M, Bydder GM, Du J. UTE imaging with simultaneous water and fat signal suppression using a time-efficient multi-spoke inversion recovery pulse sequence. Magn Reson Med. 2015 in press.
45. Weiger M, Pruessmann KP, Hennel F. MRI with zero echo time: hard versus sweep pulse excitation. Magn Reson Med. 2011; 66:379–389. [PubMed: 21381099]
46. Grodzki DM, Jakob PM, Heismann B. Ultrashort echo time imaging using pointwise encoding time reduction with radial acquisition (PETRA). Magn Reson Med. 2012; 67:510–518. [PubMed: 21721039]

47. Idiyatullin D, Corum C, Park JY, Garwood M. Fast and quiet MRI using a swept radiofrequency. J Magn Reson. 2006; 181:342–349. [PubMed: 16782371]

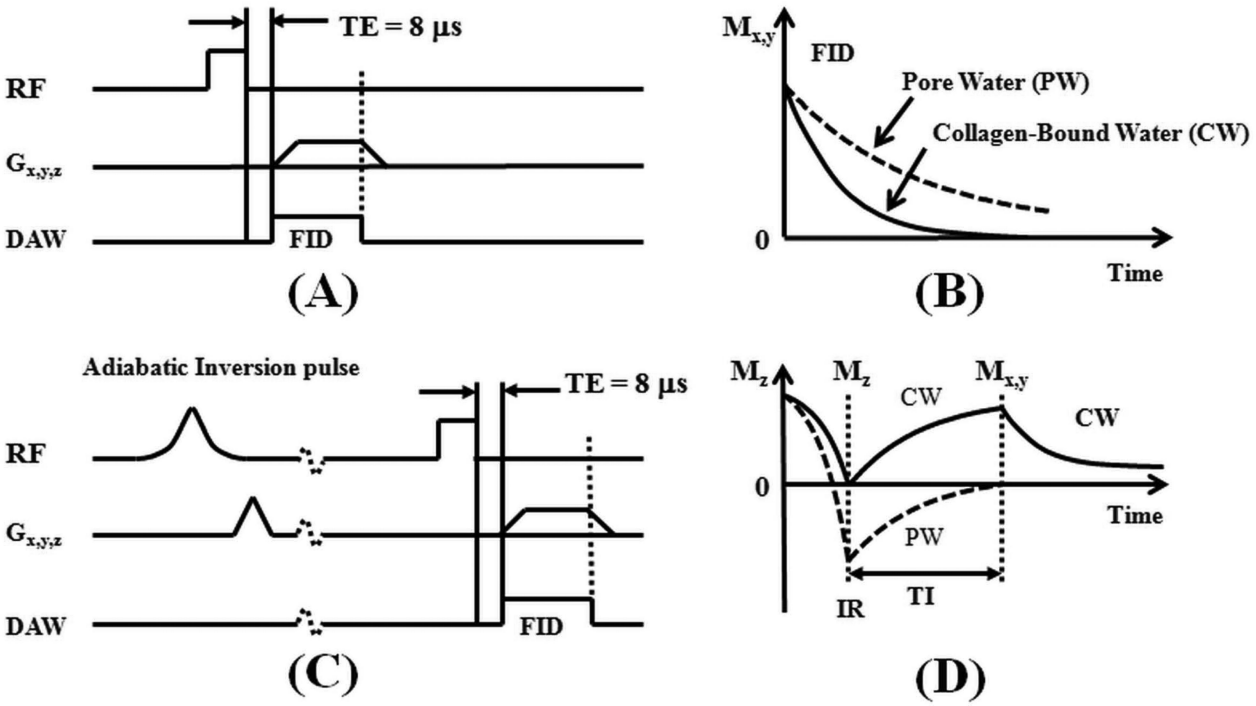

Figure 1.

The 3D UTE (A) and IR-UTE (C) sequences, as well as the contrast mechanisms for imaging of total water (B) and collagen-bound water (D). The UTE sequence employs a short rectangular pulse for signal excitation followed by 3D radial ramp sampling with a minimal nominal TE of 8 μs, which is short enough to detect signal from both collagen-bound water (CW) with very short T_2* (solid lines in B and D) and pore water (PW) with slightly longer T_2* (dashed lines in B and D). The IR-UTE sequence employs an adiabatic inversion pulse to invert and null the pore water magnetization. The collagen-bound water magnetization is not inverted and is detected by a subsequent UTE data acquisition (D). The z gradient can be turned off for fast non-selective 2D UTE and IR-UTE imaging.

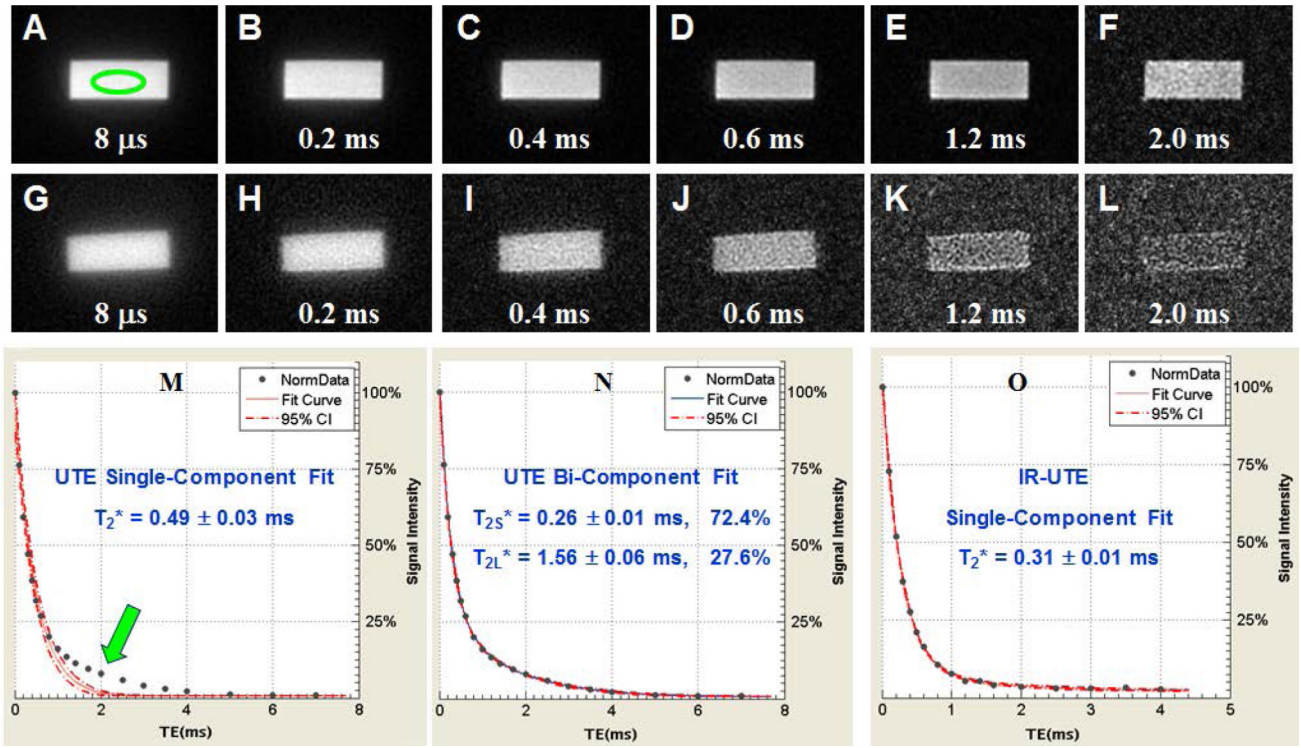

Figure 2.

Selected 2D UTE imaging of a bovine cortical bone sample with TEs of 8 μs (A), 0.2 ms (B), 0.4 ms (C), 0.6 ms (D), 0.8 ms (E), 1.6 ms (F), 2 ms (G), 3 ms (H), 4 ms (I), 5 ms (J), 6 ms (K) and 7 ms (L) as well as single component (M) and bi-component (N) fitting of the UTE images. Single component fitting of the corresponding IR-UTE images with a TR of 300 ms and TI of 90 ms was also shown (O). An ROI was drawn in (A). Single component fitting of the UTE images shows significant residual signal (> 10%) (M), which is reduced to less than 0.5% by bi-component fitting (N), which shows a shorter T_2* of 0.25 ms and a longer T_2* of 2.20 ms with respective fractions of 81.2% and 18.8% by volume. Excellent single component fitting of the IR-UTE images is achieved with residual signal less than 0.3% (O), and a T_2* of 0.30 ms which is close to that of the short T_2* component in UTE images, suggesting that bound water was detected by the IR-UTE sequence with pore water largely suppressed by the long adiabatic inversion pulse.

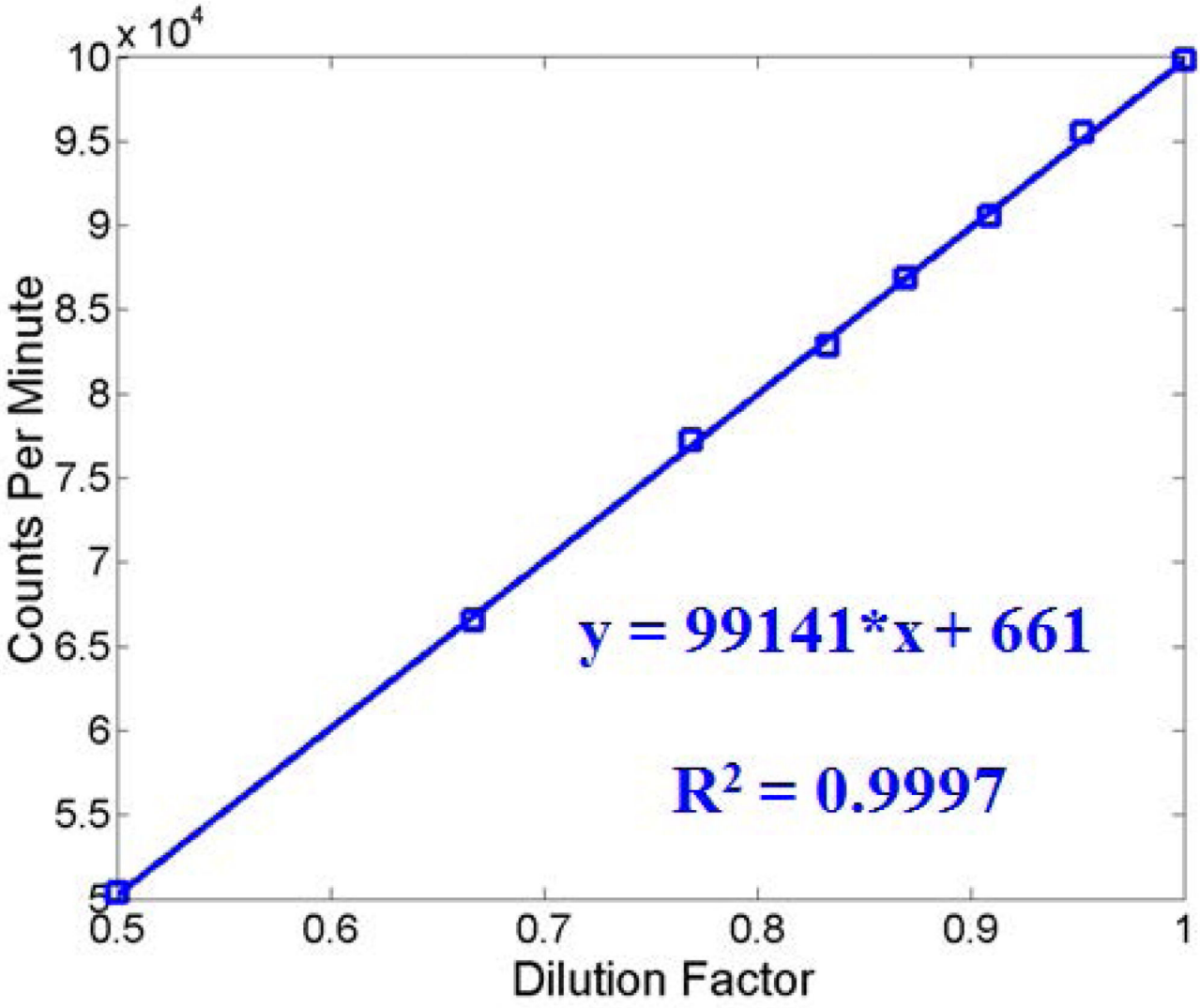

Figure 3.

T_1 measurement using saturation recovery dual echo UTE acquisitions with a TE of 8 μs (A) and 2.4 ms (B), and IR-UTE acquisitions with variable TR/TI combinations (C). A T_1^{eff} of 268 ms and fitting error of ±22 ms was measured with saturation recovery UTE acquisitions with a TE of 8 μs (A). A T_1^{pw} of 509 ms and fitting error of ±22 ms were measured with saturation recovery UTE acquisitions with a TE of 2.4 ms (B). A T_1^{CW} of 122 ms and fitting error of ±12 ms were measured with IR-UTE acquisitions with variable TR/TI combinations (C).

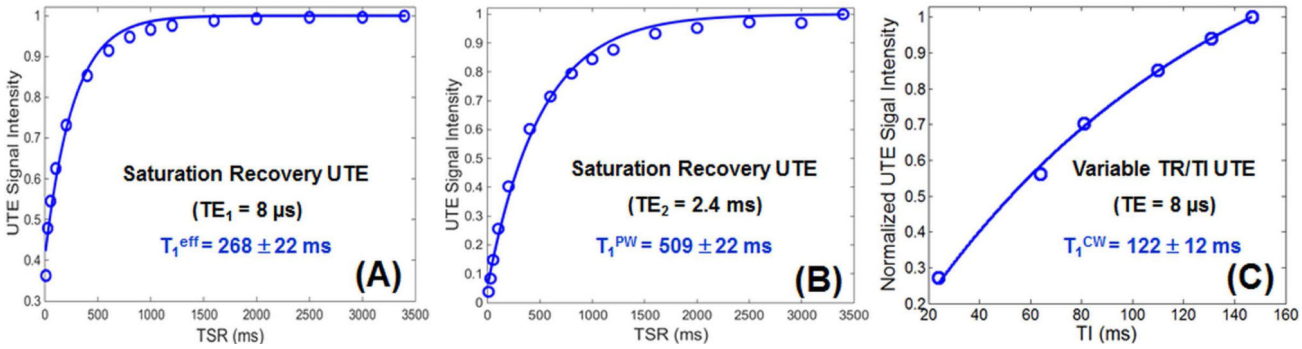

Figure 4.

Calibration curve used for THO dilution factor measurement was generated by measuring CPM as a function of THO fraction in THO/H_2O solutions. The excellent linear behavior suggests that THO dilution factors can be accurately measured via linear interpolation.

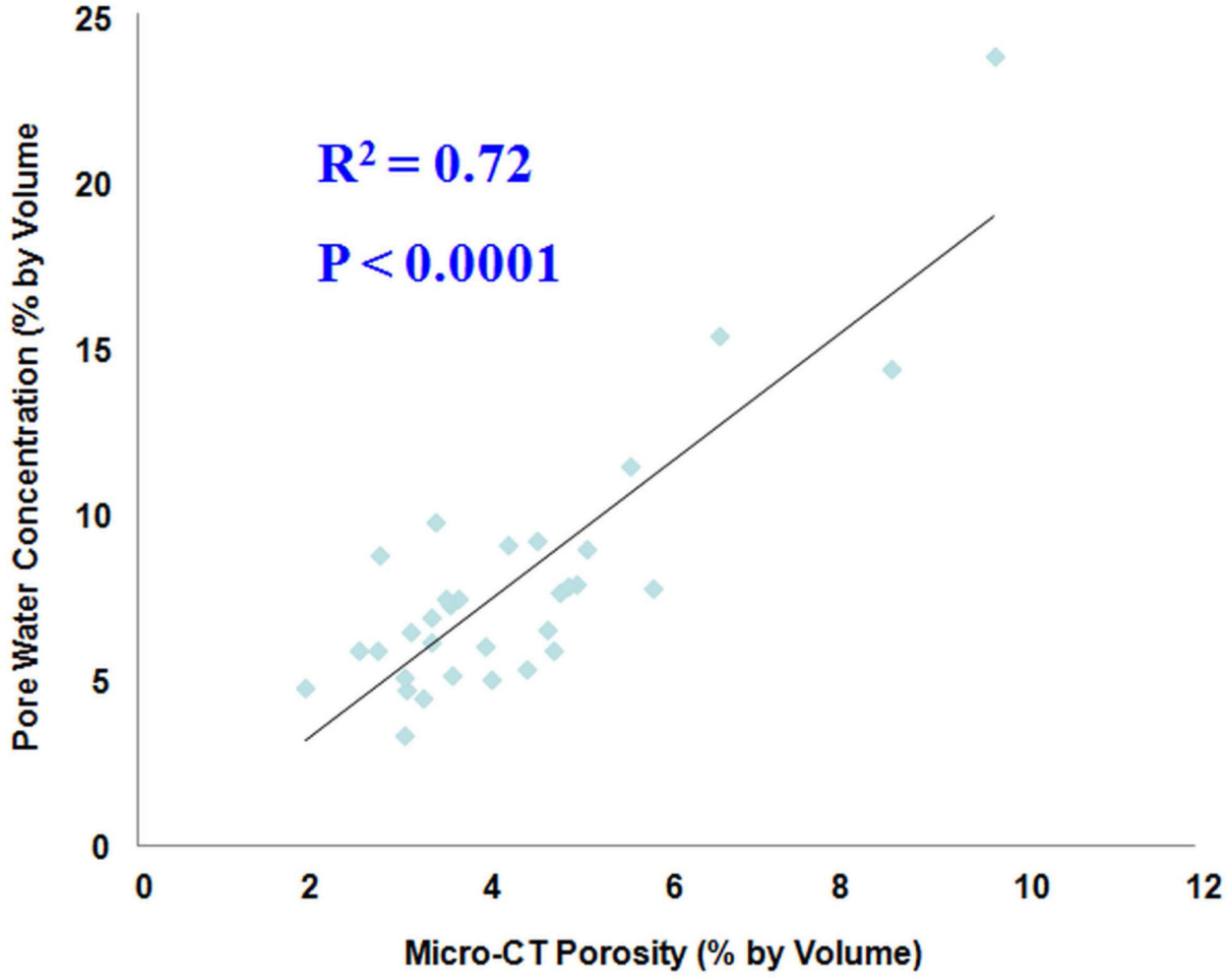

Figure 5.

Correlation between UTE measured pore water concentration and μCT porosity in cadaveric human cortical bone samples (n=32). A high correlation ($R^2 = 0.72$; $P < 0.0001$) was observed between pore water concentration and μCT porosity, suggesting that UTE sequences can reliably access water in cortical bone using a clinical MR scanner.

Table 1

Measurement of pore water T_2^* (T_2^{*pw}), collagen-bound water T_2^* (T_2^{*cw}) and total water effective T_2^* (T_2^{*eff}) using single-component and bi-component fitting of UTE images, and single-component fitting of IR-UTE images, respectively.

T_2^* Measurements	T_2^{*PW}	T_2^{*CW}	PW Fraction	CW Fraction	T_2^{*eff}
UTE Single-Component Analysis	-	-	-	-	0.41 ± 0.05 ms
UTE Bi-Component Analysis	1.84 ± 0.52 ms	0.28 ± 0.03 ms	25.4 ± 4.2%	74.6 ± 4.2%	-
IR-UTE Bi-Component Analysis	-	0.32 ± 0.02 ms	-	-	-

Table 2

Measurement of pore water T_1 (T_1^{pw}), collagen-bound water T_1 (T_1^{cw}) and total water effective T_1 (T_1^{eff}) using single-component fitting of saturation recovery dual echo UTE acquisitions with TEs of 8 μs and 2.4 ms, as well as IR-UTE acquisitions with variable TR/TI combinations and a TE of 8 μs.

T_1 Measurements	T_1^{PW}	T_1^{CW}	$T_1^{Effective}$
Saturation Recovery UTE (TE_1 = 8 μs)	-	-	243 ± 37 ms
Saturation Recovery UTE (TE_2 = 2.4 ms)	527 ± 28 ms	-	-
Inversion Recovery UTE, variable TR/TI	-	116 ± 6 ms	-

Table 3

Mean and standard deviation of pore water concentration (WC_{Pore}), collagen-bound water concentration ($WC_{Collagen}$) and mineral-bound water concentration ($WC_{Mineral}$) using UTE imaging techniques, THO-H_2O isotope exchange study and gravimetric analysis, respectively.

	Pore Water (WC_{Pore})	**Collagen-Bound Water ($WC_{Collagen}$)**	**Mineral-Bound Water ($WC_{Mineral}$)**	**WC_{Pore} + $WC_{Collagen}$**	**WC_{Pore} + $WC_{Collagen}$ + $WC_{Mineral}$**
UTE Measured WC_{Total}	-	-	-	21.0 ± 2.8%	-
IR-UTE Measured $WC_{Collagen}$	-	17.9 ± 1.6%	-	-	-
Pore Water (WC_{Total} – $WC_{Collagen}$)	4.7 ± 0.5%	-	-	-	-
UTE + Bi-Component Analysis	5.3 ± 0.4%	15.7 ± 2.3%	-	-	-
THO-H_2O Exchange	5.9 ± 0.6%	18.1 ± 2.1%	9.5 ± 0.6%	-	33.5 ± 0.6%
Gravimetric Analysis	6.3 ± 0.8%	19.2 ± 3.6%	-	25.5 ± 0.6%	-